Molecular Biology of the Cell
Vol. 15, 2335–2346, May 2004

Desmin Aggregate Formation by R120G αB-Crystallin Is Caused by Altered Filament Interactions and Is Dependent upon Network Status in Cells

Ming Der Perng,* Shu Fang Wen,* Paul van den IJssel,†‡ Alan R. Prescott,† and Roy A. Quinlan*§

*School of Biological and Biomedical Sciences, The University of Durham, Durham DH1 3LE, United Kingdom.; and †CHIPs, School of Life Sciences, Medical Science Institute, The University, Dundee DD1 5EH, Scotland

Submitted December 16, 2003; Revised February 3, 2004; Accepted February 10, 2004
Monitoring Editor: Paul Matsudaira

The R120G mutation in αB-crystallin causes desmin-related myopathy. There have been a number of mechanisms proposed to explain the disease process, from altered protein processing to loss of chaperone function. Here, we show that the mutation alters the in vitro binding characteristics of αB-crystallin for desmin filaments. The apparent dissociation constant of R120G αB-crystallin was decreased while the binding capacity was increased significantly and as a result, desmin filaments aggregated. These data suggest that the characteristic desmin aggregates seen as part of the disease histopathology can be caused by a direct, but altered interaction of R120G αB-crystallin with desmin filaments. Transfection studies show that desmin networks in different cell backgrounds are not equally affected. Desmin networks are most vulnerable when they are being made de novo and not when they are already established. Our data also clearly demonstrate the beneficial role of wild-type αB-crystallin in the formation of desmin filament networks. Collectively, our data suggest that R120G αB-crystallin directly promotes desmin filament aggregation, although this gain of a function can be repressed by some cell situations. Such circumstances in muscle could explain the late onset characteristic of the myopathies caused by mutations in αB-crystallin.

INTRODUCTION

The study of many different human diseases caused by mutations in intermediate filament (IF) proteins (McLean and Lane, 1995; Fuchs and Cleveland, 1998; Coulombe and Omary, 2002; Herrmann *et al.*, 2003) has shown that filament aggregation is a common feature (van den IJssel *et al.*, 1999), implying that 10-nm filaments need to be arranged in networks to be functional. What then determines the distribution and location of IF networks in cells? IFs are dynamic structures, individually and collectively (Helfand *et al.*, 2003). The composition of the IFs themselves is clearly a very important factor because that can influence the distribution of filaments (Cary and Klymkowsky, 1994a,b) and their dynamics (Chou *et al.*, 2003) and the effect of some intermediate filament mutations (Zhou *et al.*, 2003). The filament composition can also determine the spacing between filaments, an important part of organizing individual filaments into an ordered arrangement or network. So vimentin, but not nestin, facilitates the correct spacing of glial fibrillary acidic protein filaments (Eliasson *et al.*, 1999) and, of course, altering the proportion of the different neurofilament proteins changes the packing density of neurofilaments (Xu *et al.*, 1996). Then, the provision of appropriate docking sites, for instance on the plasma membrane (Borradori and Sonnenberg, 1999; Green and Gaudry, 2000; Garrod *et al.*, 2002), as provided by members of the spectraplakin protein family (Leung *et al.*, 2001; Roper and Brown, 2003) and also by some IF proteins themselves, such as syncoilin (Poon *et al.*, 2002). IF composition and available attachment sites are therefore important factors in network formation.

This point has been firmly made for desmin. Although previous in vitro assembly studies had shown that desmin was very capable of forming 10-nm filaments in vitro (Herrmann *et al.*, 1999) and in vivo (Raats *et al.*, 1990), the formation of a network of desmin IFs is facilitated by the presence of other IF proteins such as keratins (Schweitzer *et al.*, 2001), vimentin (Cary and Klymkowsky, 1994a,b; Schweitzer *et al.*, 2001), paranemin (Schweitzer *et al.*, 2001), and syncoilin (Poon *et al.*, 2002). Indeed, paranemin cannot form filaments independent of an appropriate assembly partner (Hemken *et al.*, 1997) such as vimentin or desmin (Schweitzer *et al.*, 2001). Syncoilin, on the other hand, does not participate directly in filament assembly but is thought to be important in anchoring desmin filaments to membrane attachment sites at the sarcolemma and neuromuscular junctions in muscle (Poon *et al.*, 2002). Keratins, too, influence the ability of desmin to form filament networks (Raats *et al.*, 1990; Schweitzer *et al.*, 2001), despite the fact that they do not seem to coassemble with desmin (Hatzfeld and Franke, 1985), suggesting again that the arrangement of assembled filaments into networks involves more than just the filament proteins themselves. At

Article published online ahead of print. Mol. Biol. Cell 10.1091/mbc.E03–12–0893. Article and publication date are available at www.molbiolcell.org/cgi/doi/10.1091/mbc.E03–12–0893.

‡ Present address: Faculteit der Geneeskunde, Kamer B334, Free University Medical Centre, Van der Boechorststraat 7, 1081 BT Amsterdam, The Netherlands.
§ Corresponding author. E-mail address: r.a.quinlan@durham.ac.uk.

Abbreviations used: DRM, desmin-related myopathy; DTT, dithiothreitol IF, intermediate filament; PMSF, phenylmethylsulfonyl fluoride; sHSP, small heat shock protein.

the very least, it shows that the surface architecture of the IF and potential docking sites available to these filaments will influence their distribution and associations (Herrmann and Aebi, 2000; Herrmann and Foisner, 2003) as they form a functional filament network.

IF dysfunction can be caused not only by mutations in IF proteins (Coulombe and Omary, 2002) but also in their associated proteins (Smith *et al*., 1996). Recently, a missense mutation R120G in αB-crystallin was confirmed as the genetic basis for a rare human desmin-related myopathy (Vicart *et al*., 1998), and this has been followed by two other αB-crystallin mutations that also cause similar myopathies (Selcen and Engel, 2003). Although these data support the previous hypothesis that small heat shock proteins (sHSPs) are important modulators of IF assemblies (Nicholl and Quinlan, 1994), it has been suggested for R120G αB-crystallin that the formation of the desmin aggregates may not be due to a direct physical or biochemical interaction between desmin and the mutant αB-crystallin (Wang *et al*., 2001; Chavez Zobel *et al*., 2003) but rather due to the loss of other αB-crystallin functions such as their ability to inhibit apoptosis (Kamradt *et al*., 2002), interact with the transcriptional machinery in the nucleus (van den IJssel *et al*., 2003), influence genome stability (Andley *et al*., 2001), or play a role in proteosome function (den Engelsman *et al*., 2003). Direct evidence to show that αB-crystallin directly contributes to desmin network formation is therefore still required as a key step in understanding the biological basis of desmin-related myopathy (DRM).

In the study presented here, we have used transient transfections and in vitro cosedimentation assays coupled with electron microscopy to investigate the effects of the R120G mutation on the role of αB-crystallin in desmin filament network formation and maintenance. Together, our data support the hypothesis that it is the direct interaction between the desmin filaments and the R120G αB-crystallin that causes desmin filament aggregates.

MATERIALS AND METHODS

Expression and Purification of Recombinant Wild-Type and Mutant αB-Crystallin

Plasmids containing wild-type and R120G αB-crystallin in the pET23b vector (Novagen, Nottingham, United Kingdom) were constructed as described previously (Perng *et al*., 1999b). The expression constructs of both wild-type and mutant αB-crystallin were transformed into *Escherichia coli* BL21 (DE3) pLysS strain. Recombinant protein expression was induced using 0.5 mM isopropyl-1-thio-β-D-galactopyranoside for 3 h once the bacterial culture had reached an OD_{600} of 0.6. The bacteria were harvested and resuspended in TEN buffer (50 mM Tris-HCl, pH 8.0, 1 mM EDTA, 100 mM NaCl, 1 mM $MgCl_2$, 0.2 mM phenylmethylsulfonyl fluoride [PMSF]) containing Complete protease inhibitor cocktail tablet (Roche Diagnostics, Indianapolis, IN) and lysed by several freeze and thaw cycles. Benzonase nuclease (Novagen) was added at a final concentration of 10 U/ml to the bacterial lysate and incubated at room temperature for 30 min. The lysate was clarified by centrifugation at 15,000 rpm in a JA-20 rotor (Beckman Coulter, High Wycombe, United Kingdom) for 30 min at 4°C, followed by filtration through a 0.2-μm filter (Whatman, Maidstone, United Kingdom). Polyethyleneimine (Sigma Chemical, Poole, Dorset, United Kingdom) was then added to the filtrate to form a 0.06% solution. After incubation on ice for 5 min, the mixture was centrifuged at 15,000 rpm for 10 min to pellet the DNA.

For wild-type and R120G αB-crystallin purification, the clear supernatant was loaded onto a DEAE-Sepharose column (Amersham Biosciences UK, Little Chalfont, Buckinghamshire, United Kingdom) preequilibrated in buffer A (20 mM Tris-HCl, pH 7.4, 20 mM NaCl, 1 mM $MgCl_2$, 1 mM EDTA, 1 mM dithiothreitol [DTT], 0.2 mM PMSF) and eluted with a linear gradient of 0–200 mM NaCl in the same buffer. The αB-crystallin–enriched fractions were pooled, concentrated, and further purified by size exclusion chromatography on a Fractogel EMD BioSEC Superformance column (60 × 1.6 cm; Merck Sharp and Dohme, Hoddesdon, United Kingdom) equilibrated in buffer B (20 mM Tri-HCl, 100 mM NaCl, pH 7.4). Purified proteins were concentrated by using Ultrafree-15 concentrator (Millipore, Watford, United Kingdom) with a 100-kDa molecular weight cut-off membrane.

Preparation of Desmin

Purified desmin was obtained by extraction of the crude intermediate filament preparation from chicken gizzards with 8 M urea and the subsequent chromatography on DEAE-cellulose (Whatman) and hydroxyapatite (Bio-Rad, Hemel Hempstead, United Kingdom) columns in the presence of 6 M urea as described in detail previously (Geisler and Weber, 1980; Huiatt *et al*., 1980). Column fractions were analyzed by SDS-PAGE, and those containing purified desmin were collected, aliquoted, and stored at −80°C. Protein concentrations were determined by the bicinchoninic acid assay (BCA reagent; Perbio Science, Chester, United Kingdom) by using bovine serum albumin as standard.

In Vitro Assembly and Cosedimentation Assay

In vitro assembly and cosedimentation assay were carried out as described previously (Perng *et al*., 1999a). Briefly, purified desmin in urea buffer (6 M urea, 20 mM Tris-HCl, pH 8.0, 1 mM EDTA, 1 mM EGTA, 1 mM DTT, 0.2 mM PMSF) was dialyzed by stepwise lowering of the urea concentration into low ionic strength buffer (10 mM Tris-HCl, pH 8.0, 1 mM DTT, 0.2 mM PMSF) at 4°C. Wild-type or mutant αB-crystallin was then mixed with desmin in low ionic strength buffer at different molar ratios as indicated. Assembly of desmin filaments in the presence or absence of αB-crystallin was initiated by addition of a 20-fold concentrated assembly buffer to give a final concentration of 100 mM imidazole-HCl, pH 6.8, 1 mM DTT, 0.2 mM PMSF. After incubation for 1 h at the indicated temperatures, protein samples were layered onto a 0.85 M sucrose cushion in the assembly buffer and centrifuged at 80,000 × *g* for 30 min at 20°C in a TL-100 Bench Top centrifuge (Beckman Coulter) by using a TLS 55 rotor (Beckman Coulter) to pellet assembled desmin filament and associated αB-crystallin. To investigate the effect of R120G mutation upon aggregate formation in vitro, desmin was assembled in the presence of wild-type or R120G αB-crystallin and subjected to a low-speed centrifugation at 3000 × *g* for 10 min in a Bench Top centrifuge (5417R; Eppendorf, Hamburg, Germany). The pellet and supernatant fractions were separated by 12% (wt/vol) SDS-PAGE and visualized by Coomassie Blue staining. The amount of protein in the supernatant and pellet fractions were analyzed by a luminescent image analyser (LAS-1000plus; Fuji Film, Tokyo, Japan) and quantified using the Image Gauge software (version 4.0; Fuji Film), by using αB-crystallin and desmin standards to determine protein amounts. The binding curve of αB-crystallin to desmin was determined by in vitro cosedimentation assay by using a fixed concentration of desmin and varying the concentration range of αB-crystallin. Scatchard analysis of these data was used to estimate the K_d for αB-crystallin binding to desmin.

Electron Microscopy

Protein samples spread on carbon-coated copper grids were negatively stained with 1% (wt/vol) uranyl acetate and examined by transmission electron microscope (Phillips 400T), by using an accelerating voltage of 80 kV. Images were captured at a magnification of 17,000× on Kodak 4489 film and then digitized at 1200 pixel^2 resolution before being processed further in Adobe Photoshop 6 (Adobe Systems, San Jose, CA).

Cell Cultures and Transient Transfection

Human adrenal cortex carcinoma cell SW13/cl.2 (kindly provided by Dr. Robert Evans, University of Colorado Health Sciences Centre, Denver, CO), human breast cancer epithelial cell MCF7, and human lens epithelial cell H36CE2 (Porter *et al*., 1998) were grown in DMEM (Sigma Chemical), supplemented with 10% (vol/vol) fetal calf serum (Sigma Chemical), 2 mM L-glutamine, and antibiotics (100 U of penicillin and 0.1 mg of streptomycin). Baby hamster kidney (BHK21) fibroblasts were grown in Glasgow minimal essential medium (Sigma Chemical) supplemented with 5% (vol/vol) tryptose phosphate broth, 5% (vol/vol) fetal calf serum, and antibiotics (100 U of penicillin and 0.1 mg/ml streptomycin). All cells were maintained at 37°C in a humidified incubator of 95% (vol/vol) air and 5% (vol/vol) CO_2.

Wild-type and R120G αB-crystallin were subcloned into a mammalian expression vector pcDNA3.1 (Invitrogen, Paisley, United Kingdom) from the bacterial expression vectors using *Nde*I and *Eco*RI restriction sites. For transfection experiments, plasmid DNA containing human desmin (kindly provided by Dr. H. Herrmann, German Cancer Research Centre, Heidelberg, Germany), wild-type, and R120G αB-crystallin in pcDNA3 (Invitrogen) was prepared using MaxiPrep kits (QIAGEN, Dorking, Surrey, United Kingdom). Cells grown on 13-mm coverslips at a density of 50–60% confluence were transiently transfected with wild-type or R120G αB-crystallin alone or cotransfected with desmin by GeneJuice transfection reagent (Novagen) according to manufacturer's protocol. Cells were allowed to recover for 48 h before processing for immunofluorescence microscopy. In some experiments, cells were treated with colcemid (Sigma Chemical) at a final concentration of 10 μM for 16 h. For observations on recovery from colcemid treatment, cells were rinsed and transferred to normal growth medium for up to 24 h.

Indirect Immunofluorescence Microscopy

For immunofluorescence studies, cells were washed twice with phosphate-buffered saline (PBS) and fixed with ice-cold methanol/acetone [1:1 (vol/vol)] for 20 min at room temperature, and washed twice with PBS containing 0.02%

(wt/vol) sodium azide and 0.02% (wt/vol) bovine serum albumin (BSA) (PBS/BSA/azide). Cells were then preblocked with 10% (vol/vol) goat serum in PBS/BSA/azide for 20 min, washed three times in PBS/BSA/azide, and then incubated with primary antibodies at room temperature for 1 h. The primary antibodies used in this study were mouse monoclonal antidesmin (1:100; D33; DakoCytomation, Ely, Cambridgeshire, United Kingdom), monoclonal anti-HSP27 (1:100; King *et al.*, 1987), monoclonal anti-αB-crystallin (1:1; Sawada *et al.*, 1993), and rabbit polyclonal antidesmin (1:100; Sigma Chemical). After washing with PBS/BSA/azide, the primary antibodies were detected using fluorescein isothiocyanate- (1:100; Jackson ImmunoResearch Laboratories, West Grove, PA) or Alexa 594 (1:800; Molecular Probes, Eugene, OR)-conjugated secondary antibodies. All antibodies were diluted in PBS/BSA/azide buffer before use. The glass coverslips were mounted on slides with the fluorescent protecting agent Citifluor (Citifluor Labs, London, United Kingdom) and observed with an Axioplan fluorescence microscope (Carl Zeiss, Jena, Germany) by using a 63× Plan-Apochromat 1.4 numerical aperture objective. Images were obtained through a cooled charge-coupled device camera (Digital Pixel, Brighton, United Kingdom) running IP Lab software. Alternatively, images were collected using an LSM 510 confocal laser scanning microscope (Carl Zeiss). Optical sections were set to ~1.0 μm. Images were processed and prepared for figures using Adobe Photoshop 7 (Adobe Systems). Quantitation of the desmin filament phenotypes was by visual assessment of the cells and scoring as cells with or without desmin containing aggregates. In cotransfection experiments, only those cells expressing both desmin and αB-crystallin were counted. Approximately 100–150 transfected cells were assessed and the experiment repeated at least three times.

Cell Fractionation and Immunoblotting

Cells plated on 75-cm² flask were washed twice with PBS before being lysed with 1 ml of extraction buffer [50 mM Tris-HCl, pH 7.4, 150 mM NaCl, 1 mM EDTA, 0.5% (vol/vol) Triton X-100] containing 1 mM PMSF and Complete protease inhibitor cocktail tablet (Roche Diagnostics). After incubation on ice for 10 min, cell lysates were removed from flasks and homogenized in a 1 ml of Dounce homogenizer. The homogenates were clarified by centrifugation at 18,000 × *g* for 10 min at 4°C in a precooled Bench Top centrifuge (Eppendorf). The resulting supernatant and pellet fractions were equalized by adding appropriate volumes of Laemmli's sample buffer (Laemmli, 1970) before SDS-PAGE and immunoblotting analysis.

Immunoblotting was performed using the semidry blotting method according to the manufacturer's specifications (Bio-Rad). After blotting, protein transfer was assessed by Ponceau S (Sigma Chemical) staining of the nitrocellulose membrane followed by destaining in Tris-buffered saline (TBS; 20 mM Tris-HCl, pH 7.4, 150 mM NaCl). After incubation with blocking solution consisting of 5% (wt/vol) dried milk powder (Marvel, Tesco Ltd., Chestnut, Herts, United Kingdom) in TBS containing 0.2% (vol/vol) Tween 20 for 2 h, the membranes were probed with a panel of antibodies, including mouse monoclonal anti-HSC70 (Hopwood *et al.*, 1997), monoclonal anti-HSP27 (ER-D5), monoclonal antidesmin (D33; DakoCytomation), monoclonal anti-actin (AC-40; Sigma Chemical), rabbit polyclonal anti-vimentin (3052), and polyclonal anti-αB-crystallin (3148) antibodies diluted to 1:1000 in blocking solution for 1 h. After several washes with TBS containing 0.2% (vol/vol) Tween 20, the membrane was incubated in horseradish peroxidase-conjugated secondary antibodies (DakoCytomation) diluted 1:1000 in blocking solution for 1 h, followed by washing with TBS for 30 min. Antibody labeling was detected by enhanced chemiluminescence using a luminescent image analyser (LAS-1000plus; Fuji Photo Film (UK), London, United Kingdom).

RESULTS

The R120G mutation in αB-crystallin caused cytoplasmic aggregates containing desmin IFs and αB-crystallin in muscle cells of affected individuals (Vicart *et al.*, 1998). Structural studies have confirmed that the R120G mutation in αB-crystallin results in altered secondary, tertiary, and quaternary structure, decreased protein stability and compromised chaperone function (Bova *et al.*, 1999; Kumar *et al.*, 1999; Perng *et al.*, 1999b). Using several in vitro assays, we determined the effects of R120G mutant upon the interaction with astrocyte-specific IF protein; glial fibrillary acidic protein had been studied previously (Perng *et al.*, 1999b). These results suggested that the major histopathological feature of the disease, namely, desmin aggregates, could result from an altered interaction between αB-crystallin and desmin. To

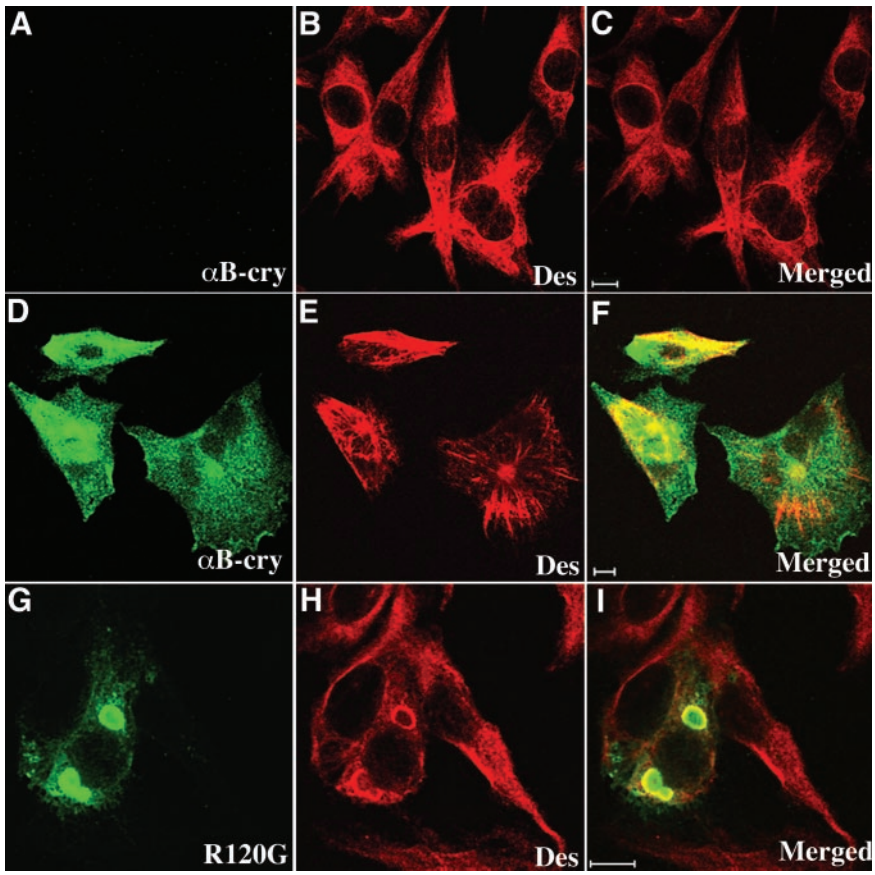

Figure 1. Formation of cytoplasmic aggregates by R120G αB-crystallin in BHK21 cells. BHK21 cells (A–C) transiently transfected with either wild-type (D–F) or R120G (G–I) αB-crystallin were fixed at 48 h posttransfection and processed for immunofluorescence microscopy as described in MATERIALS AND METHODS. Subcellular distribution of αB-crystallin and desmin were visualized by double labeling with monoclonal anti-desmin and polyclonal anti-αB-crystallin antibodies. The immunofluorescence for αB-crystallin is in the green channel (D and G), whereas the counterstaining for desmin is in the red channel (E and H). Merged images show the superimposition of the green and red signals with areas of overlap in yellow (F and I). Images were acquired by a confocal laser scanning microscope. Untransfected cells revealed extended desmin filament networks distributed throughout the cytoplasm (B), but no αB-crystallin signal can be detected (A). Cells expressing wild-type αB-crystallin showed cytoplasmic distribution of αB-crystallin (D) and desmin (E). In contrast, cells expressing R120G αB-crystallin resulted in the formation of cytoplasmic aggregates that are immuno-positive for both αB-crystallin (G) and desmin (H). Notice that desmin-positive signals were distributed outside, but not within, the aggregates (I). Bars, 10 μm.

test this hypothesis in vivo, a mammalian expression vector containing R120G αB-crystallin was generated and used to transfect in BHK21 cells. These cells were selected because they express both vimentin and desmin (Figure 1B) and contain little αB-crystallin (Figure 1A). This cell line therefore provides an opportunity to test the ability of transfected αB-crystallin constructs to affect the organization of the endogenous desmin filament networks.

BHK21 cells transfected with either wild-type or R120G αB-crystallin were fixed at 48 h posttransfection and processed for double label immunofluorescence microscopy to determine the distribution of αB-crystallin in relation to the endogenous desmin filament networks. Cells transfected with wild-type αB-crystallin showed a cytoplasmic distribution (Figure 1D) that is partially coaligned with bundles of desmin filaments (Figure 1E). In contrast, the majority of cells transfected with R120G αB-crystallin form perinuclear aggregates (Figure 1G). These aggregates were not obviously desmin positive (Figure 1, H and I), although desmin filaments were usually around the periphery of these aggregates. These data show that transfected R120G αB-crystallin leads to protein aggregate formation and the localized reorganization of desmin filament. These observations are in agreement with previously published data where desmin filaments also seemed to engulf the R120G αB-crystallin aggregates in transfected BHK21 cells (Vicart *et al.*, 1998).

To assess the relative expression levels and subcellular distributions of wild-type and R120G αB-crystallin in the presence of desmin filaments, BHK21 cells were transfected with αB-crystallin constructs before cell fractionation studies. Pellet and supernatant fractions were prepared and then probed with antibodies to desmin (Figure 2A) and αB-crystallin (Figure 2B). BHK21 cells express very low levels of endogenous αB-crystallin as shown by the immunoblot analysis of untransfected cells (Figure 2B, lanes 1 and 2). Transfection of BHK21 cells with either wild-type or R120G αB-crystallin resulted in the good expression of both proteins (Figure 2B, lanes 3–6). Whereas transfected wild-type αB-crystallin was found almost entirely in the soluble fraction (Figure 2B, lane 3), with only a small proportion present in the pellet fraction (Figure 2B, lane 4), a significant proportion (~50%) of the R120G αB-crystallin was recovered in the pellet fraction (Figure 2B, lane 6) of transfected cells. As expected, the endogenous desmin in BHK21 cells was found exclusively in the pellet fraction of both untransfected (Figure 2A, lane 2, labeled P) and transfected cells (Figure 2A, lanes 4 and 6, labeled P). Equal protein loading for each supernatant (Figure 2C, lanes 1, 3, and 5, labeled S) and pellet (Figure 2C, lanes 2, 4, and 6, labeled P) fractions were confirmed by immunoblotting for actin. These data support the proposed association between R120G αB-crystallin and desmin intermediate filaments and this association in turn could contribute directly to the reorganization of the desmin filament network seen in the R120G αB-crystallin transfected BHK21 cells.

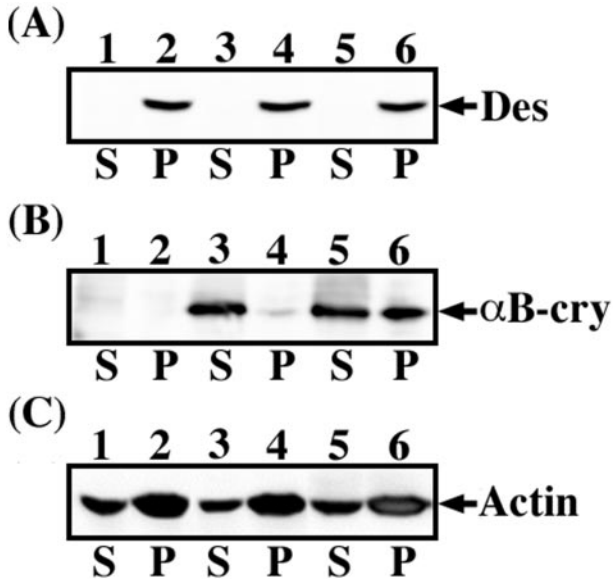

Figure 2. Immunoblotting analysis of αB-crystallin expressed in BHK21 cells. BHK21 cells were either untransfected (lanes 1 and 2) or transfected with wild-type (lanes 3 and 4) or R120G αB-crystallin (lanes 5 and 6). At 48 h posttransfection, cells were extracted with detergent buffer followed by centrifugation at 18,000 × *g* for 15 min at 4°C. The resulting supernatant (S) and pellet (P) fractions were separated by SDS-PAGE followed by immunoblotting analysis by using anti-desmin (A) and αB-crystallin (B) antibodies. The blot was developed by enhanced chemiluminescence system. Whereas wild-type αB-crystallin was present almost entirely in the soluble fraction (B, lane 3, labeled S), ~50% of R120G αB-crystallin was found in the pellet fraction (B, lane 6, labeled P). Desmin immuno-positive signals were detected exclusively in the pellet fractions (A, lanes 2, 4, and 6, labeled P). Equal loading of each supernatant and pellet fraction was confirmed by monitoring actin levels by immunoblotting with anti-actin antibody (C).

The Effect of R120G Mutation upon the Interaction with Desmin Filaments In Vitro

Cosedimentation assays were used to investigate whether wild-type and R120G αB-crystallin interacted differently with desmin filaments. In these assays, the distribution of desmin and αB-crystallin between supernatant and pellet fractions was analyzed by SDS-PAGE followed by Coomassie Blue staining and densitometry to determine protein levels. Under the conditions of the assay, desmin assembled efficiently and sedimented into the pellet fraction (Figure 3A, lanes 8, 10 and 12, labeled P) at all selected temperatures with very little (< 5%) detectable desmin left in the supernatant fractions (Figure 3A, lanes 7, 9, and 11, labeled S). In contrast, only ~10% of either wild-type or R120G αB-crystallin self-aggregated and was found in the pellet fraction (Figure 3, A and C, lanes 2, 4, and 6, respectively). When desmin and αB-crystallins were mixed at a 1:1 molar ratio, both the wild-type (Figure 3A) and R120G αB-crystallin (Figure 3C) cosedimented with desmin filaments in a temperature-dependent manner. At 22, 37, and 44°C, 8, 44, and 71%, respectively, of wild-type αB-crystallin (Figure 3B) compared with 30, 88, and 100%, respectively, of the R120G αB-crystallin (Figure 3D) cosedimented with desmin filaments. The R120G mutation therefore apparently increased the binding of αB-crystallin to desmin filaments at all temperatures, and although this binding seemed to be still temperature dependent, it was significantly greater than the maximum observed for wild-type αB-crystallin. In fact, at a 1:1 ratio the binding of R120G αB-crystallin was 100% at 44°C.

Binding curves for the interaction between either wild-type or R120G αB-crystallin with desmin were determined by measuring the ratio of bound to unbound αB-crystallin to desmin at 37°C. These ratios were calculated by measuring protein levels in the pellet and supernatant fractions obtained from the in vitro cosedimentation assays and were determined over the molar concentration range from 0.25:1 to 6:1 (Figure 4A). Representative in vitro sedimentation data are shown in Figure 3, A and C. Scatchard analysis of the binding curve data (Figure 4B) estimated the dissociation constant (K_d) for wild-type αB-crystallin as 2.45 μM, but significantly this was reduced to 1.13 μM for R120G αB-

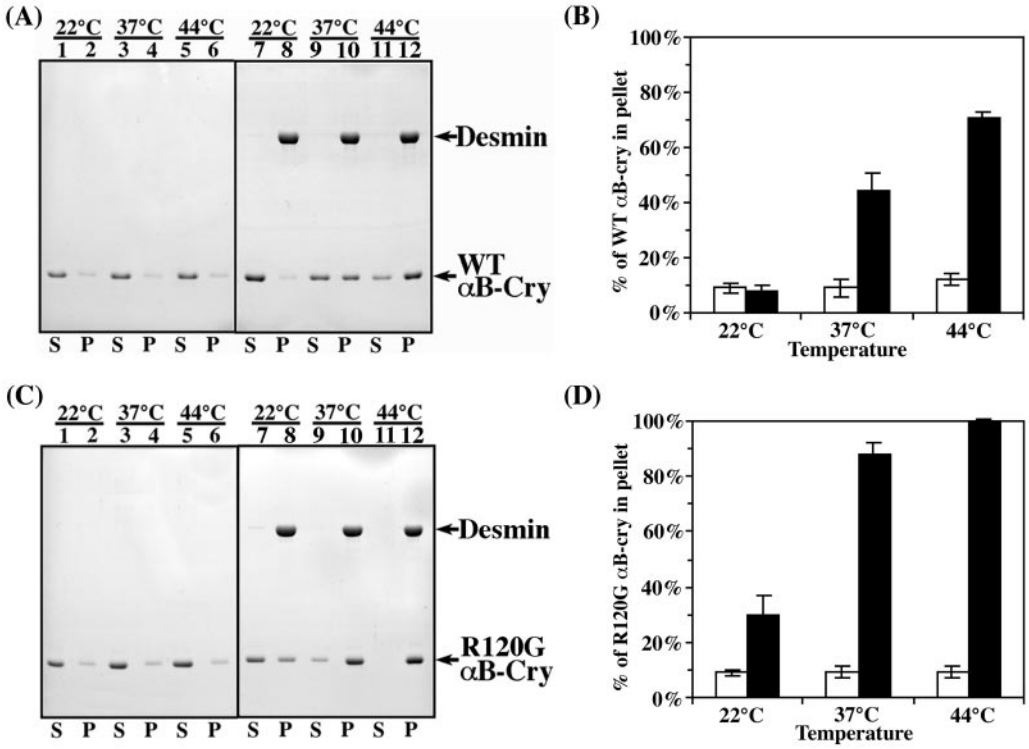

Figure 3. Cosedimentation of wild-type and R120G αB-crystallin with desmin filaments in vitro. Desmin was assembled with additions of either wild-type (A and B) or R120G αB-crystallin (C and D) at a molar ratio of 1:1 at indicated temperatures. The supernatant (S) and pellet (P) fractions were analyzed by SDS-PAGE followed by Coomassie Blue staining. The amounts of αB-crystallin and desmin in the supernatant and pellet fractions were quantified as described in MATERIALS AND METHODS. Representative gels from the cosedimentation assay are shown (A and C). The positions of desmin, wild-type and R120G αB-crystallin are indicated. Under these assay conditions, desmin assembled efficiently and more than 95% of the proteins were found in the pellet fractions (A and C; lanes 8, 10, and 12, labeled P). In the absence of desmin, both the wild-type and R120G αB-crystallin remained mostly in the supernatant (A and C; lanes 1, 3, and 5, labeled S) with only ~10% being sedimented into the pellet fractions (A and C; lanes 2, 4, and 6, labeled P). When desmin was included in the assay, both the wild-type (A) and R120G αB-crystallin (C) cosedimented with desmin filaments in a temperature-dependent manner because increasing proportions of αB-crystallin were found in the pellet fractions at elevated temperatures. The R120G αB-crystallin apparently cosedimented more efficiently than wild-type protein at all selected temperatures (cf. A and C), suggesting an increased binding of R120G αB-crystallin to desmin. Quantification results from three independent experiments are shown as mean ± SE and presented as bar charts (B and D).

crystallin. These binding data also confirm that desmin filaments can potentially bind much more R120G than wild-type αB-crystallin, which is in part due to a decreased K_d.

To visualize the in vitro association of αB-crystallin with desmin filaments, samples from the in vitro assembly were negatively stained with uranyl acetate and examined by electron microscopy. At 37°C, desmin assembled into filaments that were several micrometers in length either in the absence (Figure 5A) or presence of αB-crystallin (Figure 5, B and C). Under these assembly conditions, the presence of either wild-type (Figure 5B) or R120G αB-crystallin (Figure 5C) did not dramatically change the length of desmin filaments. Electron microscopy showed that desmin filaments in the presence of R120G αB-crystallin were heavily decorated (Figure 5C, arrows) compared with wild-type αB-crystallin (Figure 5B, arrows). These observations therefore correlated very well with the in vitro binding results (Figure 3) and their analysis (Figure 4), leading to the conclusion that the R120G mutation significantly increases the binding of αB-crystallin to desmin filaments.

One of the consequences of this increased binding could be increased interfilament interactions mediated via R120G αB-crystallin. To test this hypothesis, a low-speed centrifugation assay was developed to monitor the extent of filament–filament interactions after assembly is complete (Pollard and Cooper, 1982; Ma *et al.*, 2001). In the presence of R120G αB-crystallin, nearly all (96%) the desmin filaments were found in the pellet fraction along with 76% of the R120G αB-crystallin (Figure 6, lane 6, labeled P). By comparison, only 60% of those desmin filaments assembled in the presence of the wild-type αB-crystallin were pelleted under similar centrifugation conditions (Figure 6, lane 4, labeled P) and in this case 63% of the wild-type αB-crystallin remained in the supernatant (Figure 6, lane 3, labeled S). We interpret these data to suggest that the increased association of R120G αB-crystallin with the desmin filaments promotes more filament–filament interactions as seen by the more efficient filament sedimentation in this assay.

Cotransfection of Wild-Type αB-Crystallin Assists the Formation of Desmin Filament Networks, but R120G αB-Crystallin Prevents This Beneficial Effect

Our initial studies with BHK21 cells investigated the effect of R120G αB-crystallin upon established desmin networks. Although important, it is also necessary to consider the effect of wild-type and mutant αB-crystallin upon de novo desmin filament network formation. For this purpose, we developed a new transfection assay based on the cotransfection of αB-crystallin with desmin

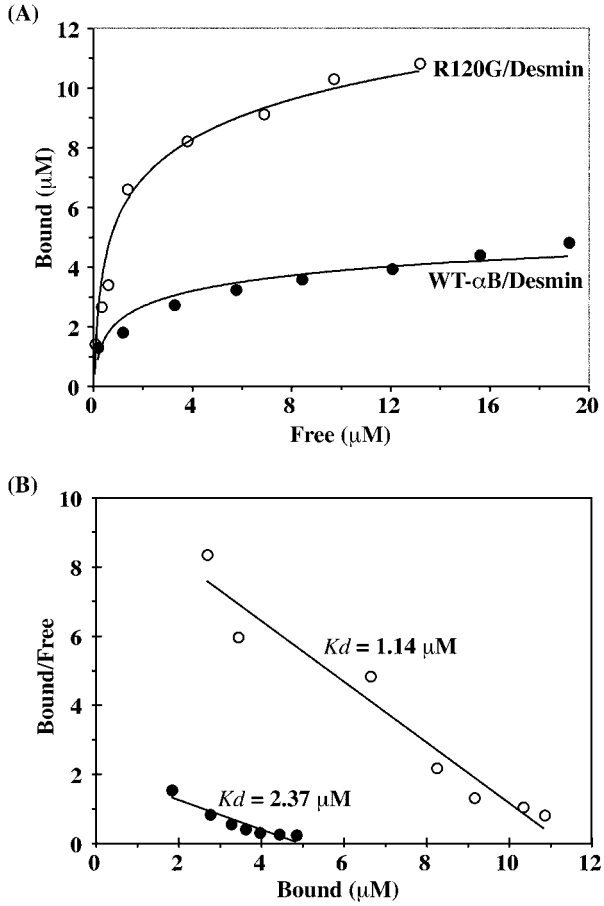

Figure 4. Binding of wild-type and R120G αB-crystallin to desmin filaments. (A) Binding curve defining the interaction between desmin and αB-crystallin. In vitro cosedimentation assay was carried out at 37°C by using a range of concentrations of αB-crystallin: desmin from 0.25:1 to 6:1. The amount of proteins in the supernatant (S) and pellet (P) fractions was quantified as described in MATERIALS AND METHODS. The data for each experiment are shown as a plot of bound versus free αB-crystallin. (B) Scatchard plots for binding of wild-type (closed circle) or R120G αB-crystallin (open circle) to desmin. The K_d of αB-crystallin and desmin interaction was obtained by converting the data as bound/free versus bound of αB-crystallin to desmin. The R120G mutant displayed a higher binding affinity (K_d = 1.14 μM) for desmin compared with wild-type αB-crystallin (K_d = 2.37 μM).

and scoring double-transfected cells for the presence of desmin-positive aggregates (Table 1).

For such an assay, it is important to determine the endogenous expression levels of αB-crystallin in these cells and of a closely related protein HSP27 because both proteins cannot only bind to and modulate intermediate filament assemblies (Nicholl and Quinlan, 1994; Perng *et al*., 1999a) but also they can prevent the aggregation of R120G αB-crystallin in transfected cells (Chavez Zobel *et al*., 2003; Ito *et al*., 2003).

Three cell lines were selected and the expression levels of the small heat shock proteins αB-crystallin and HSP27 were determined (Figure 7). Equal protein loading per lane was verified using the house-keeping protein HSC70 (Figure 7A, lanes 1–3). MCF7 and SW13/cl.2 cells have both been used before in the study of desmin network formation (Schweitzer *et al*., 2001). A human lens epithelial cell line H36 was selected because it expressed both sHSPs (Figure 7, C and D, lane 1), whereas

Table 1. Desmin aggregate formation in cells transfected with desmin alone or cotransfected with either wild type or mutant αB-crystallin

	% of Cells with desmin aggregates		
Cotransfectant with desmin	H36	SW13/cl.2	MCF7
None (desmin alone)	87 ± 3	62 ± 3	13 ± 3
WT αB-crystallin	45 ± 4	41 ± 5	10 ± 2
R120G αB-crystallin	74 ± 8	96 ± 2	55 ± 5

H36, SW13/cl.2, and MCF7 cells were cotransfected with desmin and either wild-type or R120G αB-crystallin. Cells immuno-positive for both the transfected αB-crystallin and desmin were scored for the presence of desmin-positive aggregates. The mean and standard deviation is shown as percentage ± SE and represents an average of three independent experiments. The transfection efficiency was similar for each experiment and ranged from 10 to 20%. For each experiment, ~100–150 cells were counted in random fields. Cells transfected only with desmin (none) was used as the control for these experiments.

SW13/cl.2 (Figure 7C, lane 2) and MCF7 cells (Figure 7C, lane 3) only expressed HSP27. None of the cells expressed desmin (our unpublished data) and only the H36 cell line expressed vimentin (Figure 7B, lane 1). Vimentin is a natural assembly partner for desmin (Quinlan and Franke, 1982; Schweitzer *et al*., 2001) and in a rat model of cataractogenesis, desmin can be expressed in lens epithelial cells (Lovicu *et al*., 2002) showing that desmin transfection in these cells is still a mimic of a physiologically important situation.

MCF7 cells express keratins (K8, 18, and 19), but not type III IFs (Figure 7B; Schweitzer *et al*., 2001). Despite the lack of a type III assembly partner, desmin was still able to form extensive filament networks in most (87%; Table 1) of the transfected cells (Figure 8C), which is consistent with previous studies (Raats *et al*., 1990; Schweitzer *et al*., 2001). Cotransfection of desmin with wild-type αB-crystallin had no obvious effect on desmin filament networks (Figure 8F and Table 1). In contrast, the R120G mutant had a dramatic effect on desmin filament organization when cotransfected with desmin. More than one-half of the transfected cells (55%; Table 1) contained ring-like perinuclear desmin aggregates (Figure 8I), which are morphologically distinct compared with the other cell lines (see below). These data confirm the dominant effect of R120G αB-crystallin upon aggregate formation.

We then selected another cell line, SW13/cl.2 cells, that do not contain vimentin (Figure 7B) or any other cytoplasmic intermediate filaments (Sarria *et al*., 1990) to examine the effect of αB-crystallin upon de novo filament network formation in this cell background. In agreement with previous published results (Schweitzer *et al*., 2001), desmin formed cytoplasmic aggregates with some filaments and short rod-like structures in these cells (Figure 8B). Transfection of these cells with desmin and wild-type αB-crystallin decreased the formation of aggregates (Figure 8E) from 62 to 41% (Table 1). In contrast, cells cotransfected with desmin and R120G αB-crystallin led to densely packed aggregates without any detectable filamentous staining (Figure 8H), again suggestive of a dominant effect when compared with wild-type αB-crystallin.

Desmin was then cotransfected into H36 cells with either wild-type (Figure 8D) or R120G αB-crystallin (Figure 8G). Despite the presence of αB-crystallin and HSP27 (Figure 7, C and D), the transfection of desmin alone resulted in a strong tendency to form aggregates (87%) in

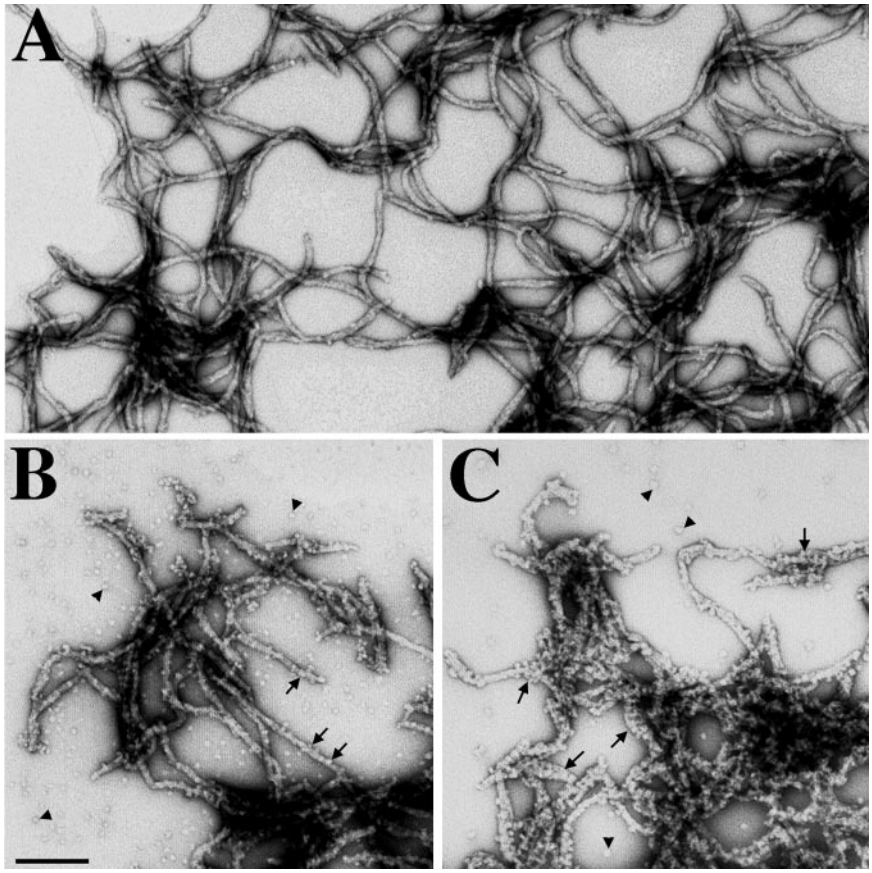

Figure 5. Visualization of wild-type and R120G αB-crystallin binding to desmin filament in vitro by electron microscopy. Desmin was assembled either alone (A) or in the presence of wild-type (B), or R120G αB-crystallin (C) at 37°C for 1 h. After assembly, protein samples were negatively stained with 1% (wt/vol) uranyl acetate and examined by electron microscopy. Under these assembly conditions, desmin formed typical 10-nm filaments with several microns in length (A). In the presence of wild-type αB-crystallin, desmin filaments had some αB-crystallin particles attached (B, arrows). In contrast, the increased binding of R120G αB-crystallin resulted in a very extensive coating of desmin filaments (C, arrows). All micrographs are at the same magnification. Bar, 200 nm.

these lens cells (Figure 8A). The ectopic overexpression of wild-type αB-crystallin seemed to significantly reduce this tendency (Figure 8D), whereas the expression of R120G αB-crystallin was unable to increase upon an already high incidence of aggregate formation (Figure 8G) when cotransfected with desmin (Table 1). From these data, two important observations emerge. First, it is clear that αB-crystallin can have a beneficial influence upon desmin filament assemblies. Second, the R120G mutation in αB-crystallin significantly inhibited this positive effect of wild-type αB-crystallin and indeed seemed to encourage desmin aggregate formation in all three different cellular backgrounds (Figure 8, G–I).

These data show that the network assembly status of desmin can greatly influence the effect of R120G αB-crystallin. These data show the effects of R120G αB-crystallin are not best seen when filament networks are in status quo, but rather when they are subjected to changes such as the formation of new networks or substantial rearrangements of existing networks. To mimic better this type of situation for preformed desmin networks, IF respreading after drug-induced collapse and recovery was used as an experimental model.

Colcemid has a well documented disrupting effect on cytoskeletal networks. The primary effect of the drug is to cause microtubule depolymerization, but after longer exposure to the drug the intermediate filament network collapses as a secondary effect. These effects are reversible by incubation of the cells in colcemid-free culture medium (Goldman *et al.*, 1979). BHK21 cells were transfected with either wild-type (Figure 9, A–F) or R120G (Figure 9, G–L) αB-crystallin and then treated for 16 h with 10 μM colcemid (Figure 9, A–C and G–I). This treatment causes the collapse of the desmin IF networks and their accumulation in the perinuclear region of the cells (Figure 9, B and H) where wild-type (Figure 9A) and R120G (Figure 9G) αB-crystallin are also concentrated. After 4 h of recovery (Figure 9, D–F and J–L), most of the desmin networks in cells expressing wild-type αB-crystallin had recovered (Figure 9E), but this was not the case in cells transfected with R120G αB-crystallin (Figure 9K). The filament aggregates and bundles were also immuno-positive for αB-crystallin, indicating that both proteins associated together in colcemid-induced collapse of the intermediate filament networks (Figure 9L).

DISCUSSION

A Direct Interaction between R120G αB-Crystallin and Desmin Leads to Aggregate Formation

Here, we have shown that the R120G mutation causes αB-crystallin to increase its binding to desmin filaments in vitro as shown by both cosedimentation assay and electron microscopy. Analysis of the cosedimentation assay data allowed us to calculate an apparent dissociation constant (K_d) for both the wild-type and R120G αB-crystallin. The values are "apparent" because both proteins are polymers, a problem previously recognized by others (Bennardini *et al.*, 1992). At the very least, we have identified an important trend relevant to understanding the disease situation. The R120G mutation in αB-crystallin causes a significant decrease in the dissociation constant and also increases the level of binding to the desmin filaments. The transfection data we have presented (Table 1 and Figure 8) also show that desmin forms aggregates with αB-crystallin when cotransfected with R120G αB-crystallin, whereas the wild-type protein facilitates desmin network formation. The recovery of cells from the drug-induced collapse of

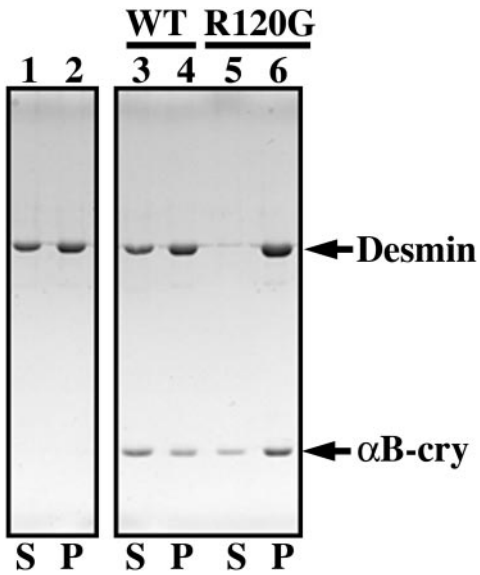

Figure 6. Increased binding of R120G αB-crystallin to desmin filaments leads to aggregate formation. Desmin was assembled in vitro (lanes 1 and 2) in the presence of either wild-type (lanes 3 and 4) or R120G (lanes 5 and 6) αB-crystallin in a molar ratio of 1:1 at 37°C for 15 min. The assembly mixtures were subjected to low-speed centrifugation at 2500 × *g* for 15 min. The resulting supernatant (S) and pellet (P) fractions were analyzed by SDS-PAGE and visualized by Coomassie Blue staining. The position of desmin and αB-crystallin are indicated. Under these assay conditions, 60% of assembled desmin filaments sedimented (lane 2), a situation that was not altered by the presence of wild-type αB-crystallin (lane 4). In the presence of R120G αB-crystallin, however, 96% of the assembled desmin filaments were pelleted (lane 6). Increased binding of R120G αB-crystallin to desmin was also observed (cf. lanes 3 and 4 with lanes 5 and 6). These data suggest that desmin assembled in the presence of R120G αB-crystallin are more easily sedimented as a result of increased filament–filament interactions.

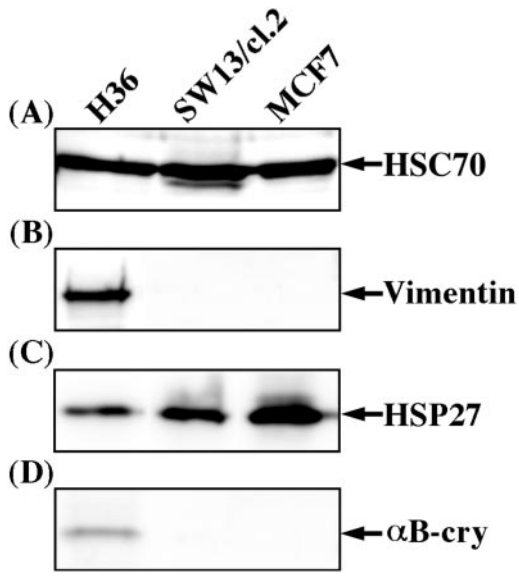

Figure 7. Expression levels of endogenous vimentin and sHSPs in different cell lines. Near confluent H36, SW13/cl.2, and MCF7 cells were extracted with detergent buffer containing 0.6 M KCl followed by centrifugation at 18,000 × *g* for 10 min at 4°C. Concentrated SDS sample buffer was then added to the cytosolic fractions and protein content ratios determined so that equivalent gel loadings from the different cell lines could be made to facilitate direct comparison of the samples. After immunoblotting, equivalent protein loadings were compared by probing with antibodies against HSC70 (A), vimentin (B), HSP27 (C), and αB-crystallin (D). Notice HSC70 levels are similar in each sample, demonstrating the equivalent protein loading and thus allowing direct comparison of the different cell extracts. H36 cells express both HSP27 and αB-crystallin, but this cell line expresses the lowest relative level of HSP27 compared with the other cell lines. Only H36 cells express vimentin, an intermediate filament protein that coassembles with desmin. MCF7 cells express the highest relative level of HSP27.

endogenous desmin filaments is also hindered by the presence of R120G αB-crystallin (Figure 9). These data not only show that the mutation has caused a gain in function by now inducing desmin filaments to aggregate and/or bundle abnormally. On the basis of these new data and the existing in vitro data (Bennardini *et al.*, 1992), we conclude that the desmin filament aggregation in the disease could involve direct binding of αB-crystallin to desmin.

Aggregation of Desmin Depends upon Network Status

DRMs caused by mutations in either the desmin or αB-crystallin gene are inherited neuromuscular disorders that are characterized by the accumulation of aggregates containing desmin and αB-crystallin (Vicart *et al.*, 1998; Goebel and Warlo, 2001; Fischer *et al.*, 2002; Goebel, 2003). Despite this direct physical association between desmin and αB-crystallin in patients with myopathy, analysis of the effects of R120G αB-crystallin in a mouse model (Wang *et al.*, 2001) and a tissue culture model (Chavez Zobel *et al.*, 2003) suggested that there was not a direct interaction between desmin and αB-crystallin. This arose because aggregates containing only R120G αB-crystallin and no desmin were found, although these were associated with IFs (Wang *et al.*, 2001; Chavez Zobel *et al.*, 2003) as has been reported for proteins accumulated in aggresome-like structures (Johnston *et al.*, 1998; Kopito, 2000).

Our results with transfected BHK21 cells (Figure 1) mirrored these events, but others presented here (Figures 8 and 9 and Table 1) help explain why the transfection (Chavez Zobel *et al.*, 2003) and transgenic models (type 1 aggregates in Wang *et al.*, 2001) led to R120G αB-crystallin aggregates that excluded endogenous IF proteins. Changes in secondary and tertiary structure do cause increased subunit association for R120G αB-crystallin (Bova *et al.*, 1999; Perng *et al.*, 1999a,b), and overexpression in tissue culture cells and muscle leads to extensive self-aggregation (Wang *et al.*, 2001; Chavez Zobel *et al.*, 2003). Our transfection data (Figures 8 and 9 and Table 1) show that to see the most dramatic effects of R120G αB-crystallin upon desmin in an overexpression system, then either new filament networks must be formed at the same time as αB-crystallin is being expressed or there must be a drastic and complete rearrangement of the IF network as demonstrated in colcemid-treated BHK21 cells. These are probable reasons why complete coaggregation of desmin and αB-crystallin was not observed by previous investigators and the phenotypes recorded did not precisely mimic typical pathology of the R120G αB-crystallin myopathy (Vicart *et al.*, 1998; Fardeau *et al.*, 2000).

Late Onset Characteristic of the Disease Linked to Specific Muscle Events

Both the human disease (Vicart *et al.*, 1998; Fardeau *et al.*, 2000) and the mouse model (Wang *et al.*, 2001) have late onset phenotypes, but both αB-crystallin (Arbustini *et al.*, 1998; Xiao and Benjamin, 1999) and desmin (Lobrinus *et al.*,

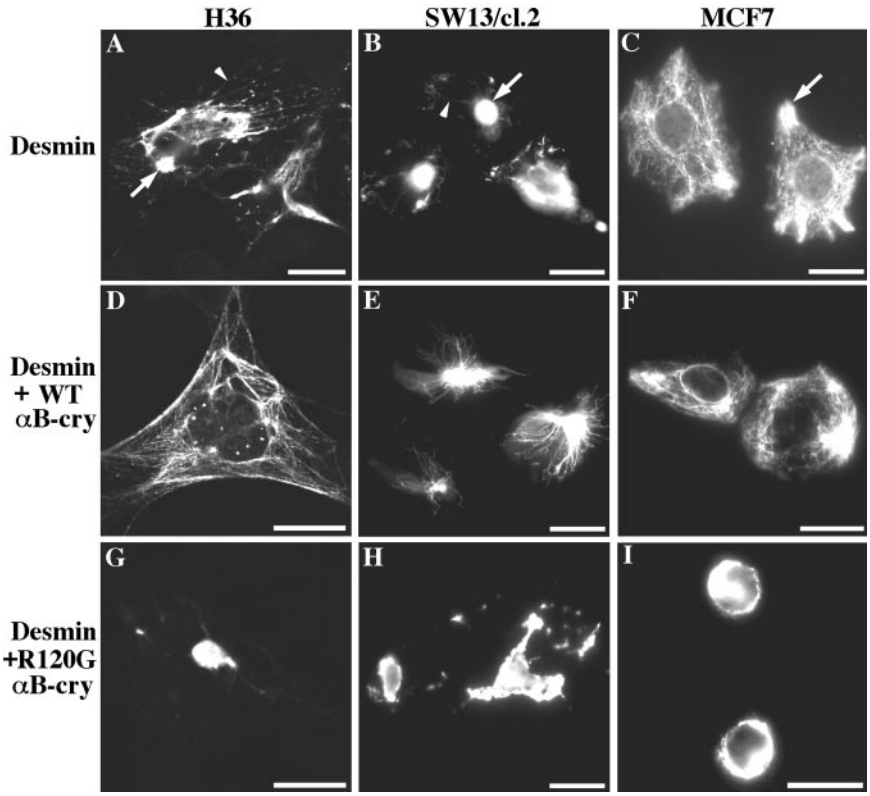

Figure 8. Effect of wild-type and R120G αB-crystallin upon desmin filament formation in vivo. H36 (A, D, and G), SW13/cl.2 (B, E, and H) and MCF7 cells (C, F, and I) were transiently transfected with desmin alone (A–C) or cotransfected with either wild-type (D–F) or R120G αB-crystallin (G–I). At 48 h posttransfection, desmin filament organizations were examined by immunostaining by using monoclonal anti-desmin antibody. In H36 cells, transfected desmin forms aggregates (A, arrow) as well as filaments (A, arrowhead). In the presence of cotransfected wild-type αB-crystallin, transfected desmin tends to form filament networks that are extended throughout the cytoplasm (D). SW13/cl.2 cells transfected with desmin form spot-like desmin aggregates (B, arrow) with some filamentous structures (B, arrowhead), but cotransfection with wild-type αB-crystallin resulted in the formation of many more extended desmin filaments in transfected cells (E). In contrast, cotransfection with R120G αB-crystallin induced large cytoplasmic desmin aggregates without any detectable filaments in both the H36 (G) and SW13/cl.2 (H) cells. In MCF7 cells, desmin formed extended filaments with some peripheral accumulations (C, arrow). Whereas cotransfection with wild-type αB-crystallin had no obvious effect on desmin filament networks (F), transfection of desmin with R120G mutant induced the formation of ring-like perinuclear desmin aggregates (I). Bars, 20 μm. Quantification of desmin network organizations in transfected cells is shown in Table 1.

1998) levels are increased during myoblast fusion. This suggests that there has to be other events occurring during muscle development to prevent both desmin aggregate formation and loss of muscle function in the patients and the transgenic mice expressing either R120G αB-crystallin or desmin mutants. Other studies have shown that chaperone proteins such as HSP27 (Ito *et al.*, 2003) and HSP70 (Chavez Zobel *et al.*, 2003) could inhibit the aggregation of R120G αB-crystallin. Our transfection studies show that the presence of other IF networks can reduce desmin aggregate formation in agreement with previous studies, e.g., Raats *et al.* (1990) and Schweitzer *et al.* (2001). Desmin is one of the earliest differentiated markers expressed in myoblasts (Furst *et al.*, 1989; Schaart *et al.*, 1989), and these cells also express synemin (Granger and Lazarides, 1980), nestin, and vimentin (Lendahl *et al.*, 1990), giving an adequate network for desmin network formation, via a coassembly mechanism (Bennett *et al.*, 1979; Gard *et al.*, 1979; Capetanaki *et al.*, 1997) during muscle development. This suggests that there are circumstances specific to mature muscle that particularly predisposes it to the effects of the αB-crystallin mutation, thus explaining the late onset characteristic of these diseases.

We have shown that any situation that induces the collapse of the endogenous desmin filament networks will make the endogenous desmin networks more prone to aggregation by R120G αB-crystallin. Other studies have shown that cell stresses such as heat shock (Morley *et al.*, 1995), osmotic shock (D'Alessandro *et al.*, 2002), or chemical stress (Ku *et al.*, 1996; Ku *et al.*, 1998) can provide the trigger to induce IF collapse and reveal the effects of IF perturbations. Indeed, stress promotes the increased association of αB-crystallin with IFs (Djabali *et al.*, 1997), and this is true, too, of muscle (Golenhofen *et al.*, 1998) where levels of αB-crystallin are increased as a result of stress (Inaguma *et al.*, 1995; Neufer and Benjamin, 1996), and there is also a stress-induced translocation of αB-crystallin to the myofibril cytoskeleton (Golenhofen *et al.*, 1998). These data suggest that any muscle stress could initiate and/or propagate the development of DRM caused by the R120G mutation in αB-crystallin.

Cardiac muscle usually responds to stress by hypertrophy (Tarone and Lembo, 2003). In the mouse model, overexpression of R120G αB-crystallin, but not wild-type αB-crystallin, also induced hypertrophy (Wang *et al.*, 2001). The hypertrophy resulted in progressive muscle failure (Wang *et al.*, 2001) typified by desmin aggregate formation and this is an example of how hypertrophy as a stress response could indeed be a potential trigger for desmin filament aggregate formation in cardiac muscle. In skeletal muscle, eccentric exercise (Yu *et al.*, 2003) induces new sarcomere formation with significant changes in desmin expression and distribution. This is another example where a physiological response later in life could initiate a sequence of events to allow pathology to develop as a result of desmin or αB-crystallin mutations. The loss of desmin filament function in cardiac and skeletal muscle myocytes is expected to affect not only mitochondrial function (reviewed in Capetanaki, 2002) but also active force generation (Balogh *et al.*, 2002) in the cardiomyocytes. Such damaging consequences make it easy to appreciate how the expression of R120G αB-crystallin could cause the developing myopathy by affecting desmin filament function.

In the transgenic mouse model of the R120G αB-crystallin-induced myopathy, it was observed that the levels of R120G αB-crystallin in cardiomyocytes increased with age (Wang *et al.*, 2001). This was not the case for wild-type protein, and it was proposed that protein degradation could be affected by the mutant αB-crystallin. Two other missense mutations in αB-crystallin that cause muscle myopathy reported increased levels of total αB-crystallin and also desmin in the affected skeletal muscles (Selcen and Engel, 2003), despite the fact that the mutant αB-crystallins were expressed at lower levels than the

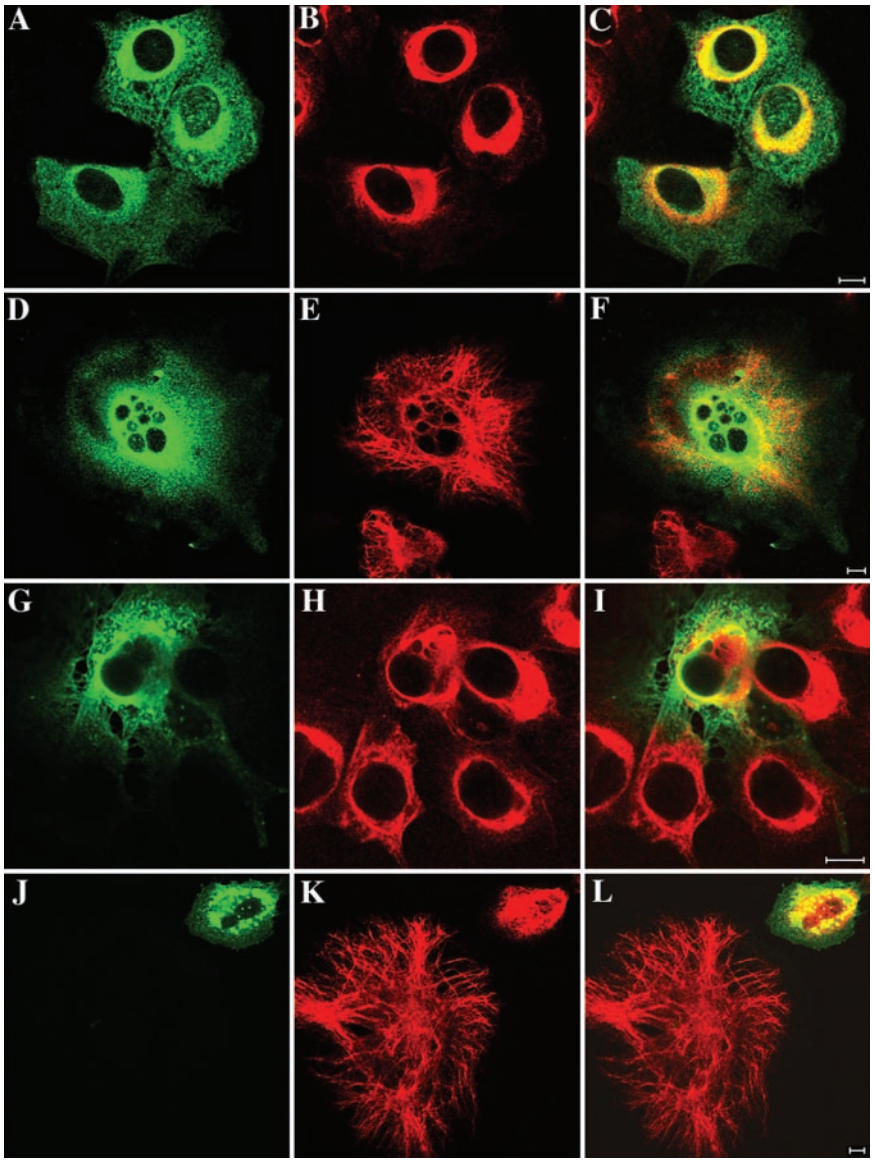

Figure 9. Distribution of desmin and αB-crystallin in colcemid-treated and recovered cells as revealed by double-label immunofluorescence microscopy. BHK21 cells transfected with either wild-type (A–F) or R120G αB-crystallin (G–L) were treated with 10 μM colcemid for 16 h. After colcemid treatment, cells were allowed to recover for 4 h in normal growth medium (D–F and J–L). Cells were then fixed and processed for double-label immunofluorescence microscopy by using monoclonal anti-desmin (B, E, H, and K) and polyclonal anti-αB-crystallin (A, D, G and J) antibodies. The distributions of desmin (red) and αB-crystallin (green) were visualized by a confocal laser scanning microscope. Merged images show the regions of colocalization between αB-crystallin and desmin appearing yellow (C, F, I and L). Notice that both wild-type and R120G αB-crystallin colocalized with collapsed desmin filaments in the perinuclear region (C, I and L). Bar, 10 μm.

wild-type αB-crystallin (Selcen and Engel, 2003), again suggestive of a compromised protein degradation system. Indeed, the protein aggregates containing the desmin and αB-crystallin were not ubiquitin labeled (Selcen and Engel, 2003), which is unusual compared with other myopathies (Goebel and Warlo, 2000; Goebel, 2003). Satellite cells isolated from patients with the R120G αB-crystallin mutation were also more susceptible to oxidative stress (Nedellec *et al.*, 2002) symptomatic of a compromised stress response. The demonstration that αB-crystallin interacts with a ubiquitin ligase component and stimulates protein ubiquitination (den Engelsman *et al.*, 2003) is very suggestive of a direct role for αB-crystallin in the ubiquitin–proteosome pathway and a link between compromised protein degradation and the developing myopathy (Hoffman, 2003).

Protein aggregate formation impairs the function of the ubiquitin–proteosome system (Bence *et al.*, 2001; Cowan *et al.*, 2003) and results in the accumulation of αB-crystallin in aggresomes (Ito *et al.*, 2002) along with IFs (Johnston *et al.*, 1998). Aggregates of desmin and αB-crystallin typify the histopathological feature of the DRMs (Goebel and Warlo, 2000; Fischer *et al.*, 2002; Goebel, 2003), and these would accompany and exacerbate compromised protein degradation in muscle cells. The compromised turnover of misfolded and/or damaged proteins would be an additional stress induced by the αB-crystallin mutations, which could either trigger or propagate the developing myopathy. Such hypotheses concerning the initiation and downstream consequences for the R120G mutation in αB-crystallin merit further investigation.

Formation of IF Networks Is Assisted by αB-Crystallin

The results from the transient transfection of desmin into three different cell lines demonstrate the ability of αB-crystallin to assist the formation of IF networks in living cells. We had previously proposed one of the functions of sHSPs is to help manage IF networks by controlling filament–filament interactions (Perng *et al.*, 1999a), and the data presented here support this proposed function for αB-crystallin, although with some qualifications. Cell background influences the ability of desmin to form networks (Table 1) and although this will be partly due to the IF expression profile of the cells (Schweitzer *et al.*, 2001), αB-crystallin is clearly

another factor in the successful formation of desmin networks in cells.

ACKNOWLEDGMENTS

We thank Dr. H. Herrmann (German Cancer Research Centre, Heidelberg, Germany) for kind gift of desmin expression construct and Dr. R.M. Evans (University of Colorado Health Sciences Centre) for generously providing SW13/cl.2 cells. We also thank John James (CHIPs, School of Life Sciences, University of Dundee) and Terry Gibbons (Biological and Biomedical Sciences, University of Durham) for excellent technical support. The financial support of the Wellcome Trust (to R.A.Q., M.D.P.; PvI, TG; 46747) and the National Institutes of Health (to R.A.Q., M.D.P., T.G., S.F.W.; NS42803) are gratefully acknowledged.

REFERENCES

Andley, U.P., Song, Z., Wawrousek, E.F., Brady, J.P., Bassnett, S., and Fleming, T.P. (2001). Lens epithelial cells derived from alphaB-crystallin knockout mice demonstrate hyperproliferation and genomic instability. FASEB J. *15*, 221–229.

Arbustini, E., *et al*. (1998). Restrictive cardiomyopathy, atrioventricular block and mild to subclinical myopathy in patients with desmin-immunoreactive material deposits. J. Am. Coll. Cardiol. *31*, 645–653.

Balogh, J., Merisckay, M., Li, Z., Paulin, D., and Arner, A. (2002). Hearts from mice lacking desmin have a myopathy with impaired active force generation and unaltered wall compliance. Cardiovasc. Res. *53*, 439–450.

Bence, N.F., Sampat, R.M., and Kopito, R.R. (2001). Impairment of the ubiquitin-proteasome system by protein aggregation. Science *292*, 1552–1555.

Bennardini, F., Wrzosek, A., and Chiesi, M. (1992). αB-crystallin in cardiac tissue: association with actin and desmin filaments. Circ. Res. *71*, 288–294.

Bennett, G.S., Fellini, S.A., Toyama, Y., and Holtzer, H. (1979). Redistribution of intermediate filament subunits during skeletal myogenesis and maturation in vitro. J. Cell Biol. *82*, 577–584.

Borradori, L., and Sonnenberg, A. (1999). Structure and function of hemidesmosomes: more than simple adhesion complexes. J. Investig. Dermatol. *112*, 411–418.

Bova, M.P., Yaron, O., Huang, Q., Ding, L., Haley, D.A., Stewart, P.L., and Horwitz, J. (1999). Mutation R120G in αB-crystallin, which is linked to a desmin-related myopathy, results in an irregular structure and defective chaperone-like function. Proc. Natl. Acad. Sci. USA *96*, 6137–6142.

Capetanaki, Y. (2002). Desmin cytoskeleton: a potential regulator of muscle mitochondrial behavior and function. Trends Cardiovasc. Med. *12*, 339–348.

Capetanaki, Y., Milner, D.J., and Weitzer, G. (1997). Desmin in muscle formation and maintenance: knockouts and consequences. Cell Struct. Funct. *22*, 103–116.

Cary, R.B., and Klymkowsky, M.W. (1994a). Desmin organization during the differentiation of the dorsal myotome in *Xenopus laevis*. Differentiation *56*, 31–38.

Cary, R.B., and Klymkowsky, M.W. (1994b). Differential organization of desmin and vimentin in muscle is due to differences in their head domains. J. Cell Biol. *126*, 445–456.

Chavez Zobel, A.T., Loranger, A., Marceau, N., Theriault, J.R., Lambert, H., and Landry, J. (2003). Distinct chaperone mechanisms can delay the formation of aggresomes by the myopathy-causing R120G alphaB-crystallin mutant. Hum. Mol. Genet. *12*, 1609–1620.

Chou, Y.H., Khuon, S., Herrmann, H., and Goldman, R.D. (2003). Nestin promotes the phosphorylation-dependent disassembly of vimentin intermediate filaments during mitosis. Mol. Biol. Cell *14*, 1468–1478.

Coulombe, P.A., and Omary, M.B. (2002). 'Hard' and 'soft' principles defining the structure, function and regulation of keratin intermediate filaments. Curr. Opin. Cell Biol. *14*, 110–122.

Cowan, K.J., Diamond, M.I., and Welch, W.J. (2003). Polyglutamine protein aggregation and toxicity are linked to the cellular stress response. Hum. Mol. Genet. *12*, 1377–1391.

D'Alessandro, M., Russell, D., Morley, S.M., Davies, A.M., and Lane, E.B. (2002). Keratin mutations of epidermolysis bullosa simplex alter the kinetics of stress response to osmotic shock. J. Cell Sci. *115*, 4341–4351.

den Engelsman, J., Keijsers, V., de Jong, W.W., and Boelens, W.C. (2003). The small heat-shock protein alpha B-crystallin promotes FBX4-dependent ubiquitination. J. Biol. Chem. *278*, 4699–4704.

Djabali, K., de Nechaud, B., Landon, F., and Portier, M.M. (1997). AlphaB-crystallin interacts with intermediate filaments in response to stress. J. Cell Sci. *110*, 2759–2769.

Eliasson, C., Sahlgren, C., Berthold, C.H., Stakeberg, J., Celis, J.E., Betsholtz, C., Eriksson, J.E., and Pekny, M. (1999). Intermediate filament protein partnership in astrocytes. J. Biol. Chem. *274*, 23996–24006.

Fardeau, M., Vicart, P., Caron, A., Chateau, D., Chevallay, M., Collin, H., Chapon, F., Duboc, D., Eymard, B., Tome, F.M., Dupret, J.M., Paulin, D., and Guicheney, P. (2000). Familial myopathy with desmin storage seen as a granulo-filamentar, electron-dense material with mutation of the alphaB-cristallin gene. Rev. Neurol. *156*, 497–504.

Fischer, D., Matten, J., Reimann, J., Bonnemann, C., and Schroder, R. (2002). Expression, localization and functional divergence of alphaB-crystallin and heat shock protein 27 in core myopathies and neurogenic atrophy. Acta Neuropathol. *104*, 297–304.

Fuchs, E., and Cleveland, D.W. (1998). A structural scaffolding of intermediate filaments in health an disease. Science *279*, 514–519.

Furst, D.O., Osborn, M., and Weber, K. (1989). Myogenesis in the mouse embryo: differential onset of expression of myogenic proteins and the involvement of titin in myofibril assembly. J. Cell Biol. *109*, 517–527.

Gard, D.L., Bell, P.B., and Lazarides, E. (1979). Coexistence of desmin and the fibroblastic intermediate filament subunit in muscle and nonmuscle cells: identification and comparative peptide analysis. Proc. Natl. Acad. Sci. USA *76*, 3894–3898.

Garrod, D.R., Merritt, A.J., and Nie, Z. (2002). Desmosomal cadherins. Curr. Opin. Cell Biol. *14*, 537–545.

Geisler, N., and Weber, K. (1980). Purification of smooth-muscle desmin and a protein-chemical comparison of desmins from chicken gizzard and hog stomach. Eur. J. Biochem. *111*, 425–433.

Goebel, H.H. (2003). Congenital myopathies at their molecular dawning. Muscle Nerve *27*, 527–548.

Goebel, H.H., and Warlo, I.A. (2000). Progress in desmin-related myopathies. J. Child Neurol. *15*, 565–572.

Goebel, H.H., and Warlo, I.A. (2001). Surplus protein myopathies. Neuromuscul. Disord. *11*, 3–6.

Goldman, R.D., Milsted, A., Schloss, J.A., Starger, J., and Yerna, M.J. (1979). Cytoplasmic fibers in mammalian cells: cytoskeletal and contractile elements. Annu. Rev. Physiol. *41*, 703–722.

Golenhofen, N., Ness, W., Koob, R., Htun, P., Schaper, W., and Drenckhahn, D. (1998). Ischemia-induced phosphorylation and translocation of stress protein alpha B-crystallin to Z lines of myocardium. Am. J. Physiol. *274*, H1457–H1464.

Granger, B.L., and Lazarides, E. (1980). Synemin: a new high molecular weight protein associated with desmin and vimentin filaments in muscle. Cell *22*, 727–738.

Green, K.J., and Gaudry, C.A. (2000). Are desmosomes more than tethers for intermediate filaments? Nat. Rev. Mol. Cell. Biol. *1*, 208–216.

Hatzfeld, M., and Franke, W.W. (1985). Pair formation and promiscuity of cytokeratin, formation in vitro heterotypic complexes and intermediate-size filaments by homologous and heterologous recombinations of purified polypeptides. J. Cell Biol. *101*, 1826–1841.

Helfand, B.T., Chang, L., and Goldman, R.D. (2003). The dynamic and motile properties of intermediate filaments. Annu. Rev. Cell Dev. Biol. *19*, 445–467.

Hemken, P.M., Bellin, R.M., Sernett, S.W., Becker, B., Huiatt, T.W., and Robson, R.M. (1997). Molecular characteristics of the novel intermediate filament protein paranemin. Sequence reveals EAP-300 and IFAPa-400 are highly homologous to paranemin. J. Biol. Chem. *272*, 32489–32499.

Herrmann, H., and Aebi, U. (2000). Intermediate filaments and their associates: multi-talented structural elements specifying cytoarchitecture and cytodynamics [In Process Citation]. Curr. Opin. Cell Biol. *12*, 79–90.

Herrmann, H., and Foisner, R. (2003). Intermediate filaments: novel assembly models and exciting new functions for nuclear lamins. Cell Mol. Life Sci. *60*, 1607–1612.

Herrmann, H., Haner, M., Brettel, M., Ku, N.O., and Aebi, U. (1999). Characterization of distinct early assembly units of different intermediate filament proteins. J. Mol. Biol. *286*, 1403–1420.

Herrmann, H., Hesse, M., Reichenzeller, M., Aebi, U., and Magin, T.M. (2003). Functional complexity of intermediate filament cytoskeletons: from structure to assembly to gene ablation. Int. Rev. Cytol. *223*, 83–175.

Hoffman, E.P. (2003). Desminopathies: good stuff lost, garbage gained, or the trashman misdirected? Muscle Nerve *27*, 643–645.

Hopwood, D., Moitra, S., Vojtesek, B., Johnston, D.A., Dillon, J.F., and Hupp, T.R. (1997). Biochemical analysis of the stress protein response in human oesophageal epithelium. Gut *41*, 156–163.

Huiatt, T.W., Robson, R.M., Arakawa, N., and Stromer, M.H. (1980). Desmin from avian smooth muscle: purification and partial characterization. J. Biol. Chem. *255*, 6981–6989.

Inaguma, Y., Hasegawa, K., Goto, S., Ito, H., and Kato, K. (1995). Induction of the synthesis of hsp27 and alpha B crystallin in tissues of heat-stressed rats and its suppression by ethanol or an alpha 1-adrenergic antagonist. J. Biochem. *117*, 1238–1243.

Ito, H., Kamei, K., Iwamoto, I., Inaguma, Y., Garcia-Mata, R., Sztul, E., and Kato, K. (2002). Inhibition of proteasomes induces accumulation, phosphorylation, and recruitment of HSP27 and alphaB-crystallin to aggresomes. J. Biochem. *131*, 593–603.

Ito, H., Kamei, K., Iwamoto, I., Inaguma, Y., Tsuzuki, M., Kishikawa, M., Shimada, A., Hosokawa, M., and Kato, K. (2003). Hsp27 suppresses the formation of inclusion bodies induced by expression of R120G alpha B-crystallin, a cause of desmin-related myopathy. Cell Mol. Life Sci. *60*, 1217–1223.

Johnston, J.A., Ward, C.L., and Kopito, R.R. (1998). Aggresomes: a cellular response to misfolded proteins. J. Cell Biol. *143*, 1883–1898.

Kamradt, M.C., Chen, F., Sam, S., and Cryns, V.L. (2002). The small heat shock protein alpha B-crystallin negatively regulates apoptosis during myogenic differentiation by inhibiting caspase-3 activation. J. Biol. Chem. *277*, 38731–38736.

King, R.J.B., Finley, J.R., Coffer, A.I., Millis, R.R., and Rubens, R.D. (1987). Characterization and biological relevance of a 29-kDa, oestrogen receptor-related protein. J. Steroid Biochem. *27*, 471–475.

Kopito, R.R. (2000). Aggresomes, inclusion bodies and protein aggregation. Trends Cell Biol. *10*, 524–530.

Ku, N.O., Michie, S.A., Soetikno, R.M., Resurreccion, E.Z., Broome, R.L., and Omary, M.B. (1998). Mutation of a major keratin phosphorylation site predisposes to hepatotoxic injury in transgenic mice. J. Cell Biol. *143*, 2023–2032.

Ku, N.O., Michie, S.A., Soetikno, R.M., Resurreccion, E.Z., Broome, R.L., Oshima, R.G., and Omary, M.B. (1996). Susceptibility to hepatotoxicity in transgenic mice that express a dominant-negative human keratin 18 mutant. J. Clin. Investig. *98*, 1034–1046.

Kumar, L.V.S., Ramakrishna, T., and Rao, C.M. (1999). Structural and functional consequences of the mutation of a conserved arginine residue in αA and αB crystallins. J. Biol. Chem. *274*, 24137–24141.

Laemmli, U.K. (1970). Cleavage of structural proteins during the assembly of the head of bacteriophage T4. Nature *227*, 680–685.

Lendahl, U., Zimmerman, L.B., and McKay, R.D. (1990). CNS stem cells express a new class of intermediate filament protein. Cell *60*, 585–595.

Leung, C.L., Liem, R.K., Parry, D.A., and Green, K.J. (2001). The plakin family. J. Cell Sci. *114*, 3409–3410.

Lobrinus, J.A., Janzer, R.C., Kuntzer, T., Matthieu, J.M., Pfend, G., Goy, J.J., and Bogousslavsky, J. (1998). Familial cardiomyopathy and distal myopathy with abnormal desmin accumulation and migration. Neuromuscul. Disord. *8*, 77–86.

Lovicu, F.J., Schulz, M.W., Hales, A.M., Vincent, L.N., Overbeek, P.A., Chamberlain, C.G., and McAvoy, J.W. (2002). TGFbeta induces morphological and molecular changes similar to human anterior subcapsular cataract. Br. J. Ophthalmol. *86*, 220–226.

Ma, L., Yamada, S., Wirtz, D., and Coulombe, P.A. (2001). A 'hot-spot' mutation alters the mechanical properties of keratin filament networks. Nat. Cell Biol. *3*, 503–506.

McLean, W.H., and Lane, E.B. (1995). Intermediate filaments in disease. Curr. Opin. Cell Biol. *7*, 118–125.

Morley, S. M., Dundas, S. R., James, J. L., Gupta, T., Brown, R. A., Sexton, C. J., Navsaria, H. A., Leigh, I. M., and Lane, E. B. (1995). Temperature sensitivity of the keratin cytoskeleton and delayed spreading of keratinocyte lines derived from EBS patients. J. Cell Sci. *108*, 3463–3471.

Nedellec, P., Edling, Y., Perret, E., Fardeau, M., and Vicart, P. (2002). Glucocorticoid treatment induces expression of small heat shock proteins in human satellite cell populations: consequences for a desmin-related myopathy involving the R120G alpha B-crystallin mutation. Neuromuscul. Disord. *12*, 457–465.

Neufer, P.D., and Benjamin, I.J. (1996). Differential expression of B-crystallin and Hsp27 in skeletal muscle during continuous contractile activity. Relationship to myogenic regulatory factors. J. Biol. Chem. *271*, 24089–24095.

Nicholl, I.D., and Quinlan, R.A. (1994). Chaperone activity of α-crystallins modulates intermediate filament assembly. EMBO J. *13*, 945–953.

Perng, M.D., Cairns, L., van den IJssel, P., Prescott, A., Hutcheson, A.M., and Quinlan, R.A. (1999a). Intermediate filament interactions can be altered by HSP27 and αB-crystallin. J. Cell Sci. *112*, 2099–2112.

Perng, M.D., Muchowski, P.J., van den IJssel, P., Wu, G.J.S., Hutcheson, A.M., Clark, K.I., and Quinlan, R.A. (1999b). The cardiomyopathy and lens cataract mutation in aB-crystallin alters its protein structure, chaperone activity and interaction with intermediate filament proteins in vitro. J. Biol. Chem. *273*, 33235–33243.

Pollard, T.D., and Cooper, J.A. (1982). Methods to characterize actin filament networks. Methods Enzymol. *85*, 211–233.

Poon, E., Howman, E.V., Newey, S.E., and Davies, K.E. (2002). Association of syncoilin and desmin: linking intermediate filament proteins to the dystrophin-associated protein complex. J. Biol. Chem. *277*, 3433–3439.

Porter, R.M., Hutcheson, A.M., Rugg, E.L., Quinlan, R.A., and Lane, E.B. (1998). cDNA cloning, expression, and assembly characteristics of mouse keratin 16. J. Biol. Chem. *273*, 32265–32272.

Quinlan, R., and Franke, W.W. (1982). Heteropolymer filaments of vimentin and desmin in vascular smooth muscle tissue and cultured baby hamster kidney cells demonstrated by chemical crosslinking. Proc. Natl. Acad. Sci. USA *79*, 3452–3456.

Raats, J.M., Pieper, F.R., Vree Egberts, W.T., Verrijp, K.N., Ramaekers, F.C., and Bloemendal, H. (1990). Assembly of amino-terminally deleted desmin in vimentin-free cells. J. Cell Biol. *111*, 1971–1985.

Roper, K., and Brown, N.H. (2003). Maintaining epithelial integrity: a function for gigantic spectraplakin isoforms in adherens junctions. J. Cell Biol. *162*, 1305–1315.

Sarria, A.J., Nordeen, S.K., and Evans, R.M. (1990). Regulated expression of vimentin cDNA in cells in the presence and absence of a preexisting vimentin filament network. J. Cell Biol. *111*, 553–565.

Sawada, K., Agata, K., Yoshiki, A., and Eguchi, G. (1993). A set of anti-crystallin mono-antibodies for detecting lens specificities-beta-crystallin as a specific marker for detecting lentoidogenesis in cultures of chicken lens epithelial cells. Jpn. J. Ophthalmol. *37*, 355–368.

Schaart, G., Viebahn, C., Langmann, W., and Ramaekers, F. (1989). Desmin and titin expression in early postimplantation mouse embryos. Development *107*, 585–596.

Schweitzer, S.C., Klymkowsky, M.W., Bellin, R.M., Robson, R.M., Capetanaki, Y., and Evans, R.M. (2001). Paranemin and the organisation of desmin filament networks. J. Cell Sci. *114*, 1079–1089.

Selcen, D., and Engel, A.G. (2003). Myofibrillar myopathy caused by novel dominant negative αB-crystallin mutations. Ann. Neurol. *54*, 804–810.

Smith, F.J., *et al*. (1996). Plectin deficiency results in muscular dystrophy with epidermolysis bullosa. Nat Genet *13*, 450–457.

Tarone, G., and Lembo, G. (2003). Molecular interplay between mechanical and humoral signalling in cardiac hypertrophy. Trends Mol. Med. *9*, 376–382.

van den IJssel, P., Norman, D.G., and Quinlan, R.A. (1999). Molecular chaperones: small heat shock proteins in the limelight. Curr. Biol. *9*, R103–R105.

van den IJssel, P., Wheelock, R., Prescott, A., Russell, P., and Quinlan, R.A. (2003). Nuclear speckle localisation of the small heat shock protein alpha B-crystallin and its inhibition by the R120G cardiomyopathy-linked mutation. Exp. Cell Res. *287*, 249–261.

Vicart, P., *et al*. (1998). A missense mutation in the αB-crystallin chaperone gene causes a desmin-related myopathy. Nature Genet. *20*, 92–95.

Wang, X., Osinska, H., Klevitsky, R., Gerdes, A.M., Nieman, M., Lorenz, J., Hewett, T., and Robbins, J. (2001). Expression of R120G αB-crystallin causes aberrant desmin and αB-crystallin aggregation and cardiomyopathy in mice. Circ. Res. *89*, 84–91.

Xiao, X., and Benjamin, I.J. (1999). Stress-response proteins in cardiovascular disease. Am. J. Hum. Genet. *64*, 685–690.

Xu, Z., Marszalek, J.R., Lee, M.K., Wong, P.C., Folmer, J., Crawford, T.O., Hsieh, S.-T., Griffin, J.W., and Cleveland, D.W. (1996). Subunit composition of neurofilaments specifies axonal diameter. J. Cell Biol. *133*, 1061–1069.

Yu, J.G., Furst, D.O., and Thornell, L.E. (2003). The mode of myofibril remodelling in human skeletal muscle affected by DOMS induced by eccentric contractions. Histochem. Cell Biol. *119*, 383–393.

Zhou, Q., Toivola, D.M., Feng, N., Greenberg, H.B., Franke, W.W., and Omary, M.B. (2003). Keratin 20 helps maintain intermediate filament organization in intestinal epithelia. Mol. Biol. Cell *14*, 2959–2971.